^{69,71}Co β-decay strength distributions from total absorption spectroscopy

S. Lyons,[1,2,*] A. Spyrou,[1,2,3] S. N. Liddick,[1,2,4] F. Naqvi,[1] B. P. Crider,[1,2,†] A. C. Dombos,[1,3,2,‡] D. L. Bleuel,[5] B. A. Brown,[1,3,2] A. Couture,[6] L. Crespo Campo,[7] J. Engel,[8] M. Guttormsen,[7] A. C. Larsen,[7] R. Lewis,[1,4] P. Möller,[9,§] S. Mosby,[6] M. R. Mumpower,[9] E. M. Ney,[8] A. Palmisano,[1,3,2] G. Perdikakis,[1,10,2] C. J. Prokop,[1,4,‖] T. Renstrøm,[7] S. Siem,[7] M. K. Smith,[1,2] and S. J. Quinn[1,3,2]

[1]*National Superconducting Cyclotron Laboratory, Michigan State University, East Lansing, Michigan 48824, USA*
[2]*The Joint Institute for Nuclear Astrophysics–Center for the Evolution of the Elements, Michigan State University, East Lansing, Michigan 48824, USA*
[3]*Department of Physics and Astronomy, Michigan State University, East Lansing, Michigan, 48824, USA*
[4]*Department of Chemistry, Michigan State University, East Lansing, Michigan, 48824, USA*
[5]*Lawrance Livermore National Laboratory, 7000 East Avenue, Livermore, California, 94550-9234, USA*
[6]*Physics Division, Los Alamos National Laboratory, Los Alamos, New Mexico, 87545, USA*
[7]*Department of Physics, University of Oslo, NO-0316, Oslo, Norway*
[8]*Department of Physics and Astronomy, University of North Carolina, Chapel Hill, North Carolina 27599, USA*
[9]*Theoretical Division, Los Alamos National Laboratory, Los Alamos, New Mexico, 87545, USA*
[10]*Central Michigan University, Mt. Pleasant, Michigan, 48859, USA*

(Received 5 November 2018; published 26 August 2019)

Background: The rapid neutron capture process is one of the main nucleosynthesis processes of elements heavier than Fe. Uncertainties in nuclear properties, such as masses, half-lives, and β-delayed neutron probabilities can cause orders of magnitude of variation within astrophysical r-process simulations. Presently, theoretical models are used to make global predictions of various nuclear properties for the thousands of nuclei required for these simulations, and measurements are required to benchmark these models, especially far from stability.
Purpose: β-decay strength distributions can be used to not only inform astrophysical r-process simulations, but also to provide a stringent test for theoretical calculations. The aim of this work is to provide accurate strength distributions for ^{69,71}Co β decay.
Method: The technique of total absorption spectroscopy was used to measure the β decay of ^{69,71}Co for the first time at the National Superconducting Cyclotron Laboratory. The ions were implanted in a double-sided silicon strip detector at the center of the Summing NaI(Tl) detector and identified using standard particle identification methods. The response of the detection system to the β-decay electron and subsequent γ-ray radiation was fit to the observed experimental data using a χ^2-minimization technique.
Results: β-feeding intensities and Gamow-Teller strength distributions were extracted from the fits of the experimental data. The β-decay intensities show that there is a large percentage of feeding to levels above 2 MeV, which have not been observed in previous studies. The resultant β-feeding intensities and Gamow-Teller strength distributions were compared to shell model and quasiparticle random phase approximation (QRPA) calculations.
Conclusions: Comparing experimentally determined β-decay strength distributions provides a test of models, which are commonly used for global β-decay properties for astrophysical calculations. This work highlights the importance of performing detailed comparisons of models to experimental data, particularly far from stability and as close to the r-process path as possible.

DOI: 10.1103/PhysRevC.100.025806

I. INTRODUCTION

The rapid neutron capture process, or r process, is known to be responsible for producing roughly half of the isotopes of the heavy elements. It occurs in neutron-rich environments where neutrons are captured in quick succession pushing nucleosynthesis towards the neutron-drip line where nuclei

*lyons@nscl.msu.edu
†Present address: Department of Physics and Astronomy, Mississippi State University, Starkville, Mississippi 39762, USA.
‡Present address: Department of Physics, University of Notre Dame, Notre Dame, Indiana, 46556, USA.
§Present Address: P. Moller Scientific Computing and Graphics, Inc. P.O. Box 1440, Los Alamos, New Mexico, 87544, USA.
‖Present address: Physics Division, Los Alamos National Laboratory, Los Alamos, New Mexico 87545, USA.

then β decay back towards stability. Though the r process has been studied since 1957, it is not yet fully understood [1–3]. For many years, two probable astrophysical sites of the r process were mainly considered: core-collapse supernovae, e.g., Refs. [4–6], and neutron-star mergers, e.g., Refs. [7,8]. However, recent observations of the kilonova that resulted from GW170817 have provided evidence that neutron-star mergers produce r-process elements [9–11]. r-process elements have also been observed in dwarf galaxies, which provides further evidence for rare events, such as neutron-star mergers, as the site of the r process [12–14]. Hence, neutron-star mergers are presently considered the main source of r-process nuclei [15], though other sites have not been ruled out.

Signatures of the r process have also been observed in metal-poor stars. Metal-poor stars provide a window into early universe nucleosynthesis as these stars essentially preserve the chemical signatures from their formation [16]. Observations of these unique stars have grown in number since the observation of CS 22892-052 (1992), which was the first metal-poor star observed with unusually strong Eu lines, a signature of r-process nucleosynthesis [17]. The composition of these stars show excellent agreement with the solar system r-process pattern for elements heavier than Ba [18]. However, for neutron-capture elements lighter than Ba, differences in the abundance pattern have been observed, for example in Barklem *et al.* [19], Honda *et al.* [20], and Roederer *et al.* [13]. Proposed reasons for these differences point to observational difficulties as well as to the possibility of additional nucleosynthesis processes that contribute to the creation of these lighter elements [18].

These differences could, in principle, be better understood by more refined r-process simulations. However, r-process simulations are sensitive to nuclear physics inputs as sensitivity studies have shown [21,22]. Uncertainties in nuclear masses, neutron-capture rates, β-delayed fission, half-lives, and neutron emission probabilities were identified as important contributors to the uncertainties in current r-process models [21–23]. Because there is a lack of experimental information for nuclei involved in the r process, some of which are not presently accessible experimentally, theoretical models are used for many of the nuclear physics inputs. More specifically, β-decay properties such as half-lives ($t_{1/2}$) and β-delayed neutron emission probabilities (P_n) can cause over an order of magnitude of variation in r-process abundances [21]. Presently, the quasiparticle random phase approximation (QRPA) is used across the nuclear chart to predict β-decay properties. These calculations are typically tested against known half-lives and β-delayed neutron emission probabilities, which are integral quantities requiring β-decay intensity (I_β) information. Therefore, a more effective test is to directly compare experimental I_β values to those used in theoretical calculations.

Traditionally, I_β is determined through β-decay measurements. Spectroscopy studies of β decay commonly use high-purity Ge detectors, which have a low efficiency causing them to often miss weak branchings to high-lying states in the daughter nucleus, resulting in low-energy β-feeding intensities to be inflated, an effect known as the pandemonium effect [24,25]. More accurate β-feeding intensities can be determined from total absorption spectroscopy (TAS) measurements, which allow nuclei far from stability to be measured, while avoiding the pandemonium effect, e.g., Refs. [26,27]. The work presented here is the first measurement of ^{69,71}Co β decay using the technique of total absorption spectroscopy.

The neutron-rich Ni isotopes, located along the $Z = 28$ shell closure and neighboring Cu and Co elements have been studied extensively to understand the interplay between simple single-particle excitations and collective behavior [28]. Both ^{69,71}Co β decays into ^{69,71}Ni have been previously studied [29–33]. Evidence of multiple isomeric states in ^{69}Co was obtained based on the differences in the β-decaying feeding pattern from ^{69}Co produced either directly through fragmentation or as a daughter product from the decay of ^{69}Fe. The high-spin β-decaying state was assumed to be the simple shell-model configuration with two neutrons in the $\nu g_{9/2}$ beyond $N = 40$. The low-spin decaying state was attributed to proton cross shell excitations and the development of a significant deformation as was also observed in ^{67}Co. Since ^{69}Co is produced in fragmentation in the present experiment, it is likely produced predominately in the high-spin configuration [33]. Suggestions of further shape coexisting states have been identified in the Co and Ni isotopes [34–38]. ^{69}Ni contains two β-decaying states: a long-lived isomeric state at 321 keV ($J^\pi = 1/2^-$, $t_{1/2} = 3.5$ s), and the ground-state ($J^\pi = 9/2^+$, $t_{1/2} = 11.4$ s) [29,30]. ^{71}Ni also exhibits two β-decaying states: a long-lived isomeric state at 499 keV ($J^\pi = 1/2^-$, $t_{1/2} = 2.3$ s), and the ground state ($J^\pi = 9/2^+$, $t_{1/2} = 2.56$ s) [39].

In the present work, the β-decay feeding intensities and Gamow-Teller strength distributions were determined from measurements of the β decay of ^{69,71}Co using the technique of total absorption spectroscopy. The next section outlines the experimental setup that was used. The subsequent analysis of the data is presented in Sec. III. Finally, the results are presented and compared to theoretical calculations commonly used in r-process models in Sec. IV.

II. EXPERIMENTAL DETAILS

The experiment was performed at the National Superconducting Cyclotron Laboratory at Michigan State University. A primary beam of ^{86}Kr at 140 MeV/nucleon was impinged on a ^{9}Be target and the fragmentation reaction products were separated in flight by the A1900 fragment separator [40] and delivered to the experimental setup. A wide momentum acceptance of the A1900 was used in order for a "cocktail" beam of isotopes around mass $A = 70$ to be delivered to the detector station. Results from the same experiment have been reported in Liddick *et al.* [41], Spyrou *et al.* [42,43], and Larsen *et al.* [44]. The isotopes of interest, ^{69,71}Co, were identified using energy loss and time-of-flight information from a plastic scintillator detector in the focal plane of the A1900 and two silicon PIN detectors that were placed upstream of the end station detector. The isotopes were implanted in a 1 mm thick double-sided silicon strip detector (DSSD), which consists of 16 vertical and horizontal strips, each 1.2 mm wide. The output of the DSSD was fed into dual gain preamplifiers,

allowing for signals from the implantation and the subsequent β-decay electrons to be read out separately [43]. The implantation and β decay were then able to be correlated in space and time allowing for the correct implantation ion to be assigned to each decay. The front and back strips of the high gain and low gain of the DSSD were gain matched using standard sources and known decay data from the experiment. Downstream of the DSSD, a silicon surface barrier detector acted as a veto detector for any ions that may have passed through the DSSD.

A front-back coincidence was implemented in hardware for the signals from the DSSD. This required that both the front and back sides of the DSSD had a signal in order to record that signal in the DSSD. This was used in order to reduce background from random noise, enabling the thresholds to be reduced, thereby increasing the β-decay detection efficiency.

The DSSD was placed at the geometric center of the Summing NaI(Tl) (SuN) detector [45]. SuN is a cylindrical 16 in. × 16 in. large volume NaI(Tl) scintillating detector with a 45 mm borehole in the center. SuN consists of eight optically isolated segments, each with three photomultiplier tubes (PMTs). The angular coverage at the center of SuN is approximately 98% and the peak efficiency for the 661 keV γ ray from ^{137}Cs is 85(2)% [45]. The signals from the eight segments are summed together to create a total absorption spectrum, which is sensitive to the total energy of the γ cascade, and therefore the level populated by β decay. In addition to the TAS spectrum, the optical isolation of the eight segments provides γ-singles spectra as well, yielding information on the deexcitation of a level by γ emission [42,46]. The multiplicity, or number of segments that detect energy during an event was determined for each decay. Before the start of the experiment the SuN PMTs were gain matched and the segments calibrated using standard ^{60}Co, ^{137}Cs, and ^{228}Th sources. To mitigate beam-induced background, a lead wall was constructed between SuN and an upstream collimator.

III. ANALYSIS

In software, implantation and β-decay events were correlated within a 1 s time window. Within this time, events meeting requirements set for an implantation event or a β-decay event were sorted allowing for further analysis.

An implantation event required a signal in both of the silicon PIN detectors, a signal in at least one strip on both sides of the DSSD in the low-gain stage, and no signal in the veto detector. The pixel of the implantation was determined by the strip with maximum energy deposited on the front and back side of the DSSD.

A decay event required no signals in either of the silicon PIN detectors, no signals in the low-gain DSSD stage, signals present in both sides of the DSSD on the high-gain stage, and no signal in the veto detector. The pixel of the decay was determined in the same way as the implantation event.

Decay events were then correlated to implantation events. To properly correlate the events, a decay event was first identified and then previous implantation events were searched for within a defined area of pixels in the DSSD. For the present work, a correlation field of one pixel was used meaning that the implant would need to have occurred in the same pixel as the decay of interest. A minimum amount of time of 1 s was required between implants to eliminate mismatching implants to the decay of interest. A correlation time window of 1 s was also used for this analysis. Using this procedure for correlating decays and implants, some of the implants will get correlated to the wrong decay resulting in random correlation events. To account for these random correlations, background spectra were created by identifying events where the decay and implant were not correlated in space. This background component was then subtracted from the data for further analysis.

In addition to random correlation background, both room background and neutron-induced background contributions were investigated. These background contributions were found to be negligible in the β-coincidence gated γ spectra, similar to what was shown previously by Dombos *et al.* [46]. The room background rate was observed at less than 3 kHz in the TAS spectra. By gating on the isotopes of interest, only the daughter decays of these nuclei would be likely contributors to the contamination of the γ spectra. To understand potential daughter contributions, daughter decay contributions were included in the half-life fitting and found not to contribute significantly ($<$1%) in both decays. While SuN is sensitive to neutrons, significant neutron background was not observed in the β-gated spectrum. This would be expected at energies 6.8MeV and above, with a strong low-energy component, as shown in Ref. [27]. Furthermore, the P_n values are expected to be small. For ^{69}Co no P_n measurement exists [47] and for ^{71}Co it is of the order of $<$3%, though there are presently conflicting results in the literature [31,48]. With such low probabilities and the low efficiency for neutron detection in SuN, background from the β-delayed neutrons is unlikely to be observed. In addition, γ rays from the deexcitation of the neutron daughters were not observed.

^{69,71}Co isotopes were identified and confirmed by their half-lives and expected γ-ray spectra. The half-lives were confirmed by fitting the decay curve with an exponential decay function plus a background constant. The half-life for ^{69}Co was previously determined for this data set by Spyrou *et al.* [43] to be 216(15) ms, which is in agreement with previous literature values [29,49–52]. The extracted half-life for ^{71}Co was determined to be 86(10) ms, which is also in good agreement with literature values [31,32,39,53]. The expected γ rays were confirmed in the singles (segment) spectra and the level energies they originate from were confirmed in the TAS spectrum.

For each isotope of interest, a procedure similar to that described in Dombos *et al.* [46] was used to determine β-decay intensities. As in that work, a combination of a folding procedure and χ^2 minimization were used to determine the β-decay intensities. The β-feeding intensities were extracted from a fit to three experimental spectra: the total absorption spectrum, the sum-of-segments spectrum, and the multiplicity spectrum.

The folding procedure requires the known level scheme to be simulated using a SuN detector simulation in GEANT4. The simulation has been previously verified with known sources and well-known resonances from ^{27}Al(p, γ)^{28}Si [45] and was modified to include the added components of the present

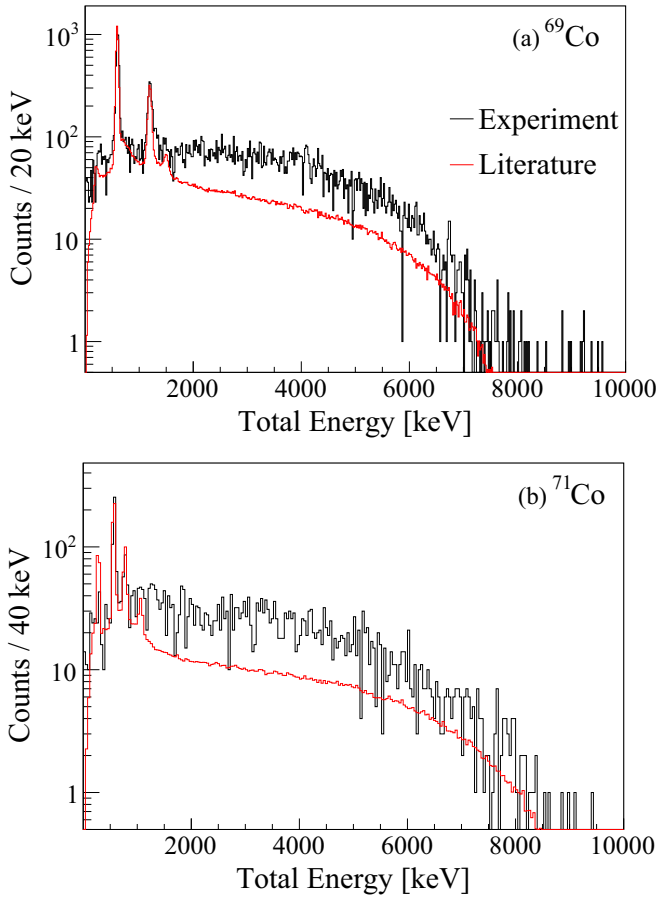

FIG. 1. Total absorption spectra for ^{69,71}Co β decay shown in black, with the SuN response simulation using only the previously known levels and decay information shown in red [55,56]. The data shown have been random background subtracted. The top figure, (a), shows the initial results for ^{69}Co and the bottom figure, (b), shows the initial results for ^{71}Co, which in this case were fit to the experimental data due to a lack of I_β values in present literature.

experiment (DSSD, veto detector, etc.). The modifications used for β-decay events have been detailed [54]. For each of the known levels of ^{69,71}Ni, simulations of the expected SuN response were produced from information available in ENSDF [55,56]. The high Q_β values, ^{69}Co (9.81 MeV) and ^{71}Co (11.33 MeV), allows for a large energy range to be populated through β decay. The data of both of the isotopes was fit using the known level schemes, however, because the level schemes for these nuclei are only known up to a few MeV, the experimental spectra could not be properly described, as shown in Fig. 1.

The deficiency at high energies seen in Fig. 1 provides evidence that previous measurements may have been affected by the pandemonium effect. Therefore to accurately fit the data, so-called pseudolevels were constructed using the statistical model code DICEBOX [57]. The ground-state spin and parity of both ^{69,71}Co is $(7/2^-)$ and therefore the spins and parities of the entry state in the daughter nucleus that were considered were $(5/2^-, 7/2^-, 9/2^-)$ assuming allowed Gamow-Teller transitions. For each of the possible spin and parity states, cascades based on input from the nuclear level density and γ-ray strength functions were modeled for specific entry state energies. The energy of the pseudolevel does not represent an actual level energy, but rather represents an energy band equivalent to the energy resolution of SuN. The DICEBOX output for each of the pseudolevels was then simulated in the SuN GEANT4 simulation. For ^{69}Co, 43 pseudolevels were constructed from 1.9–8.5 MeV. For ^{71}Co, 47 pseudolevels were constructed from 1.3–8.0 MeV. Spacing of the psuedolevels was determined using the energy resolution in SuN, leading to more psuedolevels at lower energy. Levels above S_n were considered because the data showed possible feeding to this energy range. The simulations produced the TAS, sum-of-segments, and multiplicity spectra for each of the pseudolevels. The three spectra generated for both the known levels and pseudolevels were used to simultaneously fit the same three experimental spectra in a global χ^2 minimization, where the weight of each level was the only parameter allowed to vary. This weight parameter is then used to the determine the I_β for each level.

IV. RESULTS

The resultant best fits from the χ^2 minimization are shown for ^{69}Co (Fig. 2) and ^{71}Co (Fig. 3) decay. Both show good agreement between the fit and the data. Because both ^{69,71}Ni have long-lived isomeric states, these had to be taken into consideration in the analysis. In each event window of 300 ns, all of the energy deposited into the SuN detector is summed together to create the total absorption spectra. Therefore, if a state has a lifetime longer than that, or if it β decays in that time, then the total energy will be reduced and therefore not correspond to the excitation energy of the level populated. It is also possible that from the same level, some of the cascades feed the ground state, and some feed the isomeric state, in which case for the same level you can get two sum peaks in the spectrum. These scenarios were taken into account in the analysis since the long-lived levels were included in the level scheme used for both ^{69,71}Ni.

In ^{69}Ni, the existence of a long-lived β-decaying isomer at 321 keV(3.5 s) shifts the total absorption spectra by this amount in energy if the cascade proceeds through this level. The 321 keV state has a spin and parity of $(1/2^-)$, making a β-decay transition to this state outside of the allowed Gamow-Teller transitions. Similarly, ^{71}Ni also has a long-lived isomer at 499 keV (2.3 s), which also causes an energy shift in the total absorption spectrum for all levels that decay to the isomeric state. There are two known levels in ^{71}Ni that decay directly to the ground state, 813 keV and 280.5 keV, which are observed in the total absorption spectrum at the expected energies. The decays of the long-lived isomeric states for ^{69,71}Ni were not observed in the present data.

From the best fits, the β-decay feeding intensities were extracted. The results are shown in Fig. 4 (black lines). The uncertainties (green band) for the ^{69}Co decay range from 5–20 % across the range of γ energies. For the ^{71}Co decay the uncertainty ranges from 10–30 % up to γ-ray energies of 8 MeV. The uncertainty was determined from combining the uncertainty derived from the fitting procedure and the

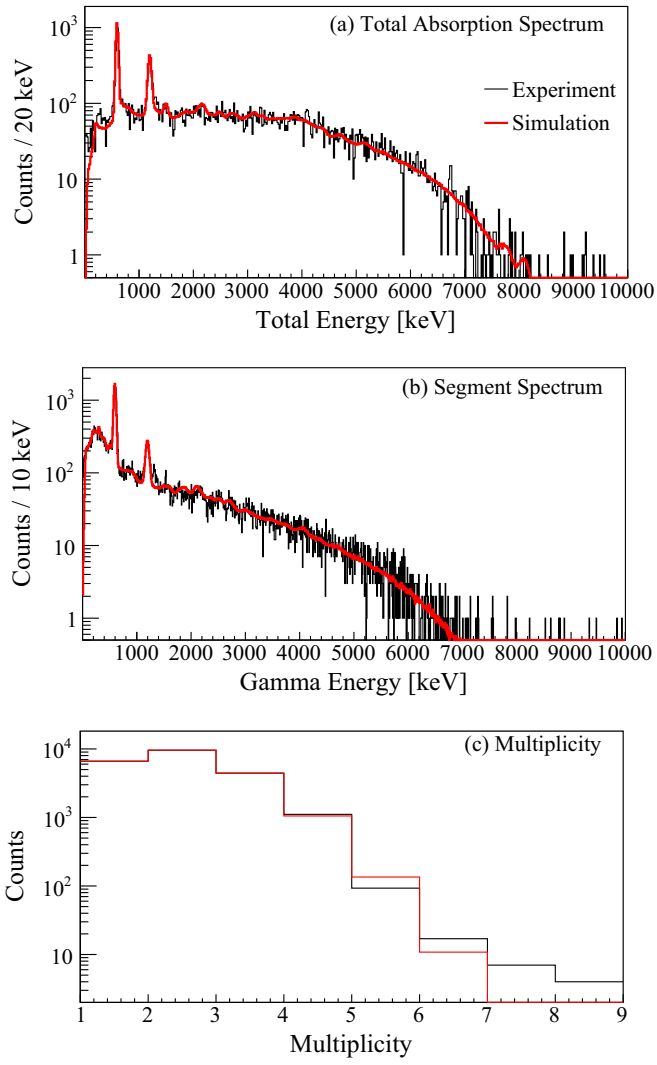

FIG. 2. Best fit achieved from the χ^2-minimization procedure for ^{69}Co. The black lines are the experimental data and the red lines shows the best fit. The top figure (a) shows the total absorption spectrum; the middle figure (b) shows the sum-of-segments spectrum; and the bottom figure (c) shows the multiplicity. The experimental spectra were gated on ^{69}Co implanted ions, and background was subtracted for random correlations.

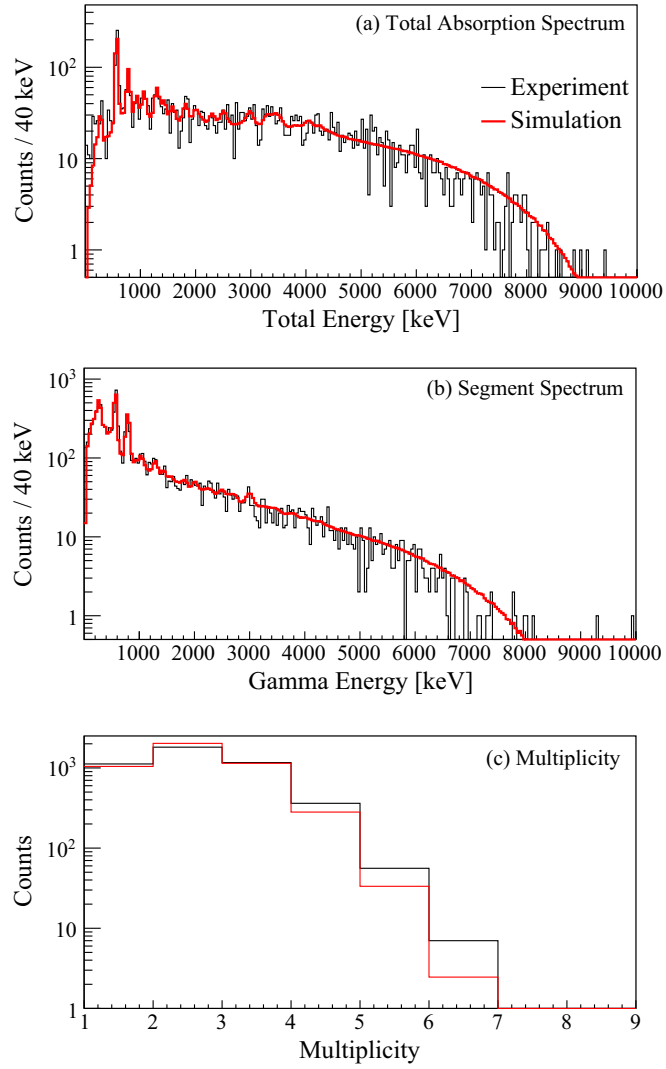

FIG. 3. Best fit for ^{71}Co. Once again, the black lines are the experimental data and the red lines shows the best fit. The top figure (a) shows the total absorption spectrum; the middle figure (b) shows the sum-of-segments spectrum; and the bottom figure (c) shows the multiplicity. The experimental spectra were gated on ^{71}Co implanted ions, and background was subtracted for random correlations.

statistical uncertainty from the counts in the total absorption spectra. For both decays, the statistical uncertainty is the main contributor to the overall uncertainty.

The cumulative β intensities in Fig. 4 are compared to three theoretical models. The long-dashed blue lines show results of QRPA calculations performed using the standard method detailed in Möller *et al.* [58] using ground-state deformations, ^{69}Co $\epsilon_2 = 0.03$ and ^{71}Co $\epsilon_2 = 0.05$, from FRDM [59]. These calculations only include allowed Gamow-Teller transitions. The double-dot-dash pink line shows the result of a fully self-consistent Skyrme QRPA calculation, obtained by applying the finite amplitude method (FAM) [60,61], extended to odd-A nuclei in the equal filling approximation [62]. The Skyrme functional and single-particle space are the same as used in the global calculation of Mustonen and Engel [63], which fixed a single set of parameters, including an effective axial-vector coupling constant g_A of 1.0, to compute the rates of even-even nuclei across the entire isotopic chart. The HFB calculation that precedes the QRPA here yields ground-state quadrupole-deformation parameters $\beta = 0.047$ in ^{69}Co, and $\beta = 0.79$ in ^{71}Co. The Skyrme QRPA calculations include a negligible forbidden contribution. The short-dashed red lines show the results of shell-model calculations, which were carried out in the $0f_{7/2}$, $0f_{5/2}$, $1p_{3/2}$, $1p_{1/2}$, $0g_{9/2}$, $0g_{7/2}$ model space. The GPFX1A Hamiltonian [64] was used for the $0f - 1p$ part of this model space. The part of the Hamiltonian involving the $0g$ orbitals was obtained from the N^{3}LO interaction [65] renormalized by V_{lowk} into six major oscillator shells and then renormalized up to second order in perturbation theory into the model space [66]. The single-particle energies were determined from the low-lying spectra and relative

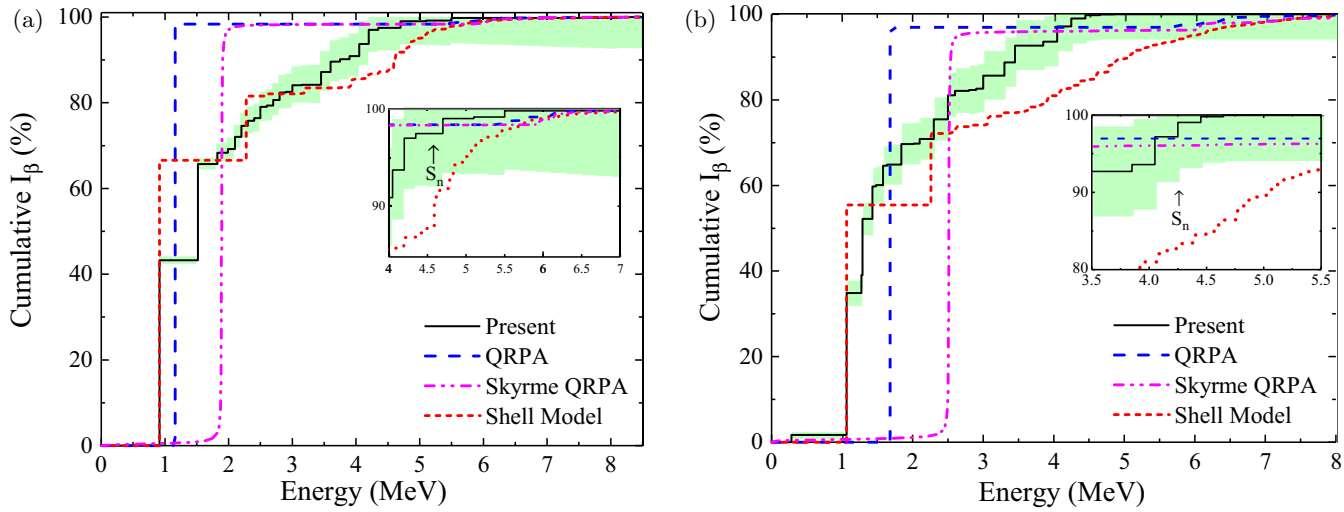

FIG. 4. Cumulative I_β shown as the black solid line with a green uncertainty band. Results are compared to QRPA calculations, shown as the long-dashed blue line, Skyrme QRPA calculations, shown as the pink double-dot-dashed line, and shell-model calculations, shown as the short-dashed red line. The insets are focused on the S_n of the daughter nucleus, ^{69,71}Ni, respectively, highlighting the intensity that competes with neutron emission. (a) Cumulative I_β results for ^{69}Co decay and (b) Cumulative I_β results for ^{71}Co decay.

binding energies of ^{69,70}Ni, ^{69}Co, and ^{71}Cu. For the spin-orbit pairs that are active in the assumed model space, the proton $0g_{9/2} - 0g_{7/2}$ spin-orbit splitting was 6.6 MeV, and the neutron $0f_{7/2} - 0f_{5/2}$ spin-orbit splitting was 6.1 MeV. Starting with a $0f_{7/2}$ proton closed-shell configuration, the lowest 5^- proton particle-hole state in ^{70}Ni comes at about 3.5 MeV. The initial ^{69,71}Co $7/2^-$ states were taken to have the configurations $C(\nu 0g_{9/2})^n(\pi 0f_{7/2})^{-1}$, where $n = 2$ for ^{69}Co and $n = 4$ for ^{71}Co. C is the closed-shell configuration $(\nu 0f_{5/2})^6(\nu 1p_{3/2})^4(\nu 1p_{1/2})^2(\pi 0f_{7/2})^8$. The ^{69,71}Ni final states were obtained from all possible one-particle one-hole $(1p - 1h)$ configurations relative to ^{69,71}Co. These final states are needed to obtain the Gamow-Teller sum-rule strength of $3(N - Z)$. To compare to the present data a quenching factor of 0.75 was used for the Gamow-Teller operator [67]. The first-forbidden transitions strengths, such as for the decays to the $9/2^+$ ground states of ^{69,71}Ni, were assumed to be small compared to the allowed Gamow-Teller strengths, and therefore were not calculated for comparison to the present data. This was further verified by including the ground-state transitions in the fitting procedure for both nuclei. The resultant contributions of these transitions were found to be up to 5% for ^{69}Co decay and up to 0.05% for ^{71}Co decay.

Comparing the present data to the QRPA calculations shown in Fig. 4, QRPA shows strong feeding at around 1 MeV in ^{69}Co decay, which is in agreement with the experimental results, though the intensity is overpredicted. The QRPA results are similar for ^{71}Co decay with a large portion of the total intensity populating a low-lying state at 1.6 MeV, which is slightly higher in energy compared to the present measurement. The Skyrme QRPA results are similar, with strong feeding near 2 MeV in ^{69}Co decay. Once again the intensity is overpredicted. For the decay of ^{71}Co most of the intensity is a higher energy, 2.5 MeV, than the experimental data and the QRPA calculations. The fragmentation of feeding to higher energies is missing in both the QRPA and Skyrme QRPA calculations.

The insets of Fig. 4 highlight the small amount of feeding above S_n in the present work. In both decays only 2–3 % of the intensity is observed above S_n. As previously discussed, there is little experimental information available on the expected P_n value, but a significant emission probability could shift the high-energy portion of the intensity. However, based on shell-model calculations, the overlap between the states populated in β decay and states in the neutron daughter are small. Therefore the decay is not expected to lead to significant n emission. The shell-model calculations are in agreement with feeding above S_n for the ^{69}Co decay, but overpredicts this feeding in the ^{71}Co decay. At present, n-γ competition is thought to be due to structure effects [42] in the region and has been observed to have a strong dependence on the spin [68,69]. Further measurements in this region would allow for the systematic study of these effects and improve the predictability of n-γ competition, which would be valuable input for r-process calculations.

The cumulative β intensities were used to calculate the Gamow-Teller strength distribution in units of $[g_A^2/4\pi]$ for each nucleus using:

$$B(\mathrm{GT}, E) = K\left(\frac{g_V}{g_A}\right)^2 \frac{I_\beta(E)}{f(Q_\beta - E)t_{1/2}}, \qquad (1)$$

where $K = 6143.6(17)$ s [70], $g_V/g_A = -1.2695(29)$ [71], $I_\beta(E)$ is the β-feeding intensity for a given energy, and f is the Fermi integral at an energy determined by the difference between the ground-state to ground-state Q_β and the given energy, E. The Fermi integrals were calculated numerically [72].

The resultant cumulative Gamow-Teller strength distributions are shown in Fig. 5 with the present results in black and the uncertainties in the green band. QRPA, Skyrme QRPA, and shell-model results are also shown in the same line style

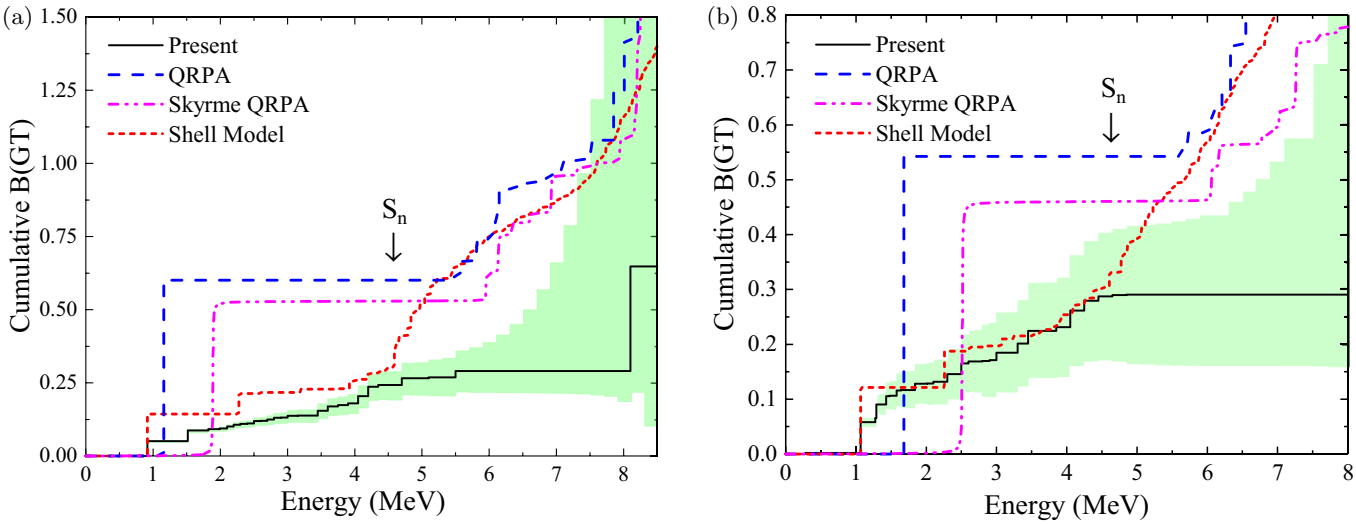

FIG. 5. Cumulative Gamow-Teller strengths shown as the black solid line with a green uncertainty band. Results are compared to QRPA calculations, shown as the long-dashed blue line, Skyrme QRPA calculations, shown as the pink double-dot-dashed line, and shell-model calculations, shown as the short-dashed red line. The present results above 5 MeV in both decays should be taken as lower limits. (a) Cumulative B(GT) results for ^{69}Co decay and (b) Cumulative B(GT) results for ^{71}Co decay.

and color as in Fig. 4. From Eq. (1) it can be seen that the strength distribution is sensitive to the energy, such that even small contributions to the intensity at higher energies have a strong B(GT) value. For energies greater than 5 MeV for both ^{69,71}Co decays, the lack of β-feeding intensity in the present work yields a constant B(GT) value and corresponding uncertainty. The strengths above 5 MeV for both nuclei should be considered as lower limits to the cumulative B(GT).

The Gamow-Teller strength starts with the $5/2^-$ state of ^{69,71}Ni. It is dominated by the $\nu 0f_{5/2}$ to $\pi 0f_{7/2}$ transition to $C(\nu 0f_{5/2})^{-1}(\nu 0g_{9/2})^n$. The gradual rise starting at 5 MeV in the shell model is dominated by $\nu 0p$ to $\pi 0p$, $\nu 0f_{5/2}$ to $\pi 0f_{5/2}$ and $\nu 0g_{9/2}$ to $\pi 0g_{9/2}$, leading to proton particle-hole states in ^{69,71}Ni. The giant Gamow-Teller resonance peak is near 19 MeV and is dominated by $\nu 0f_{7/2}$ to $\pi 0f_{5/2}$ and $\nu 0g_{9/2}$ to $\pi 0g_{7/2}$ transitions. As with the cumulative β intensities, QRPA and Skyrme QRPA overpredict the data. Shell-model calculations are in good agreement with the present B(GT) values up to S_n of the daughter nuclei in both decays. This is to be expected as the shell-model calculations use experimental information from the low-lying level scheme to constrain the calculations. Above the S_n of the daughter nuclei, the shell model predicts a continuous fragmentation of I_β, which results in significant contribution to the B(GT) at these higher energies. However, this stronger feeding was not observed in the present work. This may indicate β-delayed neutron emission for these nuclei that the present experiment was not sensitive to.

To further compare these models, the predicted half-lives that each model determines are compared in Table I. As was previously discussed, the half-lives determined in the present work are in agreement with literature values. For the half-life of ^{69}Co, the QRPA calculation is a factor of four smaller than the experimentally determined value. The Skyrme QRPA half-life is closer to the experimental value, but still not in agreement. Finally, the shell model calculates a half-life that is approximately 60% of the experimental value. For the half-life of ^{71}Co, the QRPA calculation predicts a half-life that is roughly half of the experimental value. The Skyrme QRPA calculations overpredict the half-life slightly. Shell-model calculations are very close to the experimental half-life, within 10 ms. These results along with the comparison of the β-strength distributions demonstrates how more rigorous comparisons between experiment and models can determine deficiencies, which can then be improved to progress our predictive capabilities.

TABLE I. Resultant half-lives from the present work, literature, and various models used to compare the present work.

	^{69}Co $t_{1/2}$ [ms]	^{71}Co $t_{1/2}$ [ms]
Present	216 (15)	86 (10)
ENSDF	227 (11)[a]	80 (3)[b]
QRPA	55.2	41.9
Skyrme QRPA	163.4	110.9
Shell Model	135.5	73.9

[a]Reference: Nesaraja [55].
[b]Reference: Abusaleem and Singh [56].

V. CONCLUSIONS

The β decay of ^{69,71}Co has been measured for the first time using the technique of total absorption spectroscopy at the National Superconducting Cyclotron Laboratory. The high Q_β values of these nuclei offer the unique capability to be able to make these measurements over a wide range of energies. The β-feeding intensities and Gamow-Teller strength distributions were determined from the data and compared to two theoretical models. QRPA calculations agree with the data at low energy, however, the fragmentation of the intensities at higher energies were not reproduced. Shell-model calculations were

in good agreement with the present data. A 2–3 % feeding intensity above the neutron separation energy of the daughter nuclei was observed in both nuclei. The feeding is not as strong as previously observed in neighboring nuclei, which leads to other open questions regarding the mechanism that drives these effects and their implications on n-γ competition. This competition could have an impact on r-process nucleosynthesis as it would reduce the amount of neutrons available for further n capture. The present work also demonstrates the necessity to benchmark theoretical models, particularly those used to globally calculate nuclear properties for the r process.

ACKNOWLEDGMENTS

We gratefully acknowledge the support of NSCL operations staff. This work was supported by the National Science Foundation under Grants No. PHY 1102511 (NSCL), No. PHY 1811855, No. PHY 1430152 (Joint Institute for Nuclear Astrophysics), and No. PHY 1350234 (CAREER). This material is based upon work supported by the Department of Energy/National Nuclear Security Administration through the Nuclear Science and Security Consortium under Award No. DE-NA0003180. Financial support from the Research Council of Norway, Project Grant No. 205528 (A.C.L. and M.G.) and Project Grant No. 210007 (L.C.C., T.R., and S.S.) is gratefully acknowledged. A.C.L. acknowledges funding through the ERC-STG-2014 under Grant Agreement No. 637686. D.L.B. acknowledges the support of LLNL under Contract No. DE-AC52-07NA27344. The LANL work was carried out under the auspices of the NNSA of the US Department of Energy at Los Alamos National Laboratory under Contract No. DE-AC52-06NA25396. This work was also supported by NNSA Grants No. DE-NA0000979, No. DE-NA0002132, and No. DE-NA0003221.

[1] E. M. Burbidge, G. R. Burbidge, W. A. Fowler, and F. Hoyle, Rev. Mod. Phys. **29**, 547 (1957).
[2] A. G. W. Cameron, Publ. Astron. Soc. Pac. **69**, 201 (1957).
[3] M. Arnould, S. Goriely, and K. Takahashi, Phys. Rep. **450**, 97 (2007).
[4] S. E. Woosley, J. R. Wilson, G. J. Mathews, R. D. Hoffman, and B. S. Meyer, Astrophys. J. **433**, 229 (1994).
[5] T. Fischer, S. C. Whitehouse, A. Mezzacappa, F.-K. Thielemann, and M. Liebendörfer, Astron. Astrophys. **517**, A80 (2010).
[6] L. Hüdepohl, B. Müller, H.-T. Janka, A. Marek, and G. G. Raffelt, Phys. Rev. Lett. **104**, 251101 (2010).
[7] D. Kasen, N. R. Badnell, and J. Barnes, Astrophys. J. **774**, 25 (2013).
[8] S. Wanajo, Y. Sekiguchi, N. Nishimura, K. Kiuchi, K. Kyutoku, and M. Shibata, Astrophys. J., Lett. **789**, L39 (2014).
[9] D. Kasen, B. Metzger, J. Barnes, E. Quataert, and E. Ramirez-Ruiz, Nature (London) **551**, 80 (2017).
[10] E. Troja, L. Piro, H. van Eerten, R. Wollaeger, M. Im, O. Fox, N. Butler, S. Cenko, T. Sakamoto, C. Fryer *et al.*, Nature (London) **551**, 71 (2017).
[11] E. Pian, P. D'Avanzo, S. Benetti, M. Branchesi, E. Brocato, S. Campana, E. Cappellaro, S. Covino, V. D'Elia, J. Fynbo *et al.*, Nature (London) **551**, 67 (2017).
[12] C. Sneden, J. J. Cowan, and R. Gallino, Annu. Rev. Astron. Astrophys. **46**, 241 (2008).
[13] I. U. Roederer, J. J. Cowan, A. I. Karakas, K.-L. Kratz, M. Lugaro, J. Simmerer, K. Farouqi, and C. Sneden, Astrophys. J. **724**, 975 (2010).
[14] A. P. Ji, A. Frebel, A. Chiti, and J. D. Simon, Nature (London) **531**, 610 (2016).
[15] E. Caffau, A. J. Gallagher, P. Bonifacio, M. Spite, S. Duffau, F. Spite, L. Monaco, and L. Sbordone, Astron. Astrophys. **614**, A68 (2018).
[16] A. Frebel and J. E. Norris, Metal-poor stars and the chemical enrichment of the universe, in *Planets, Stars and Stellar Systems: Galactic Structure and Stellar Populations*, edited by T. D. Oswalt and G. Gilmore (Springer, Dordrecht, 2013), Vol. 5, pp. 58–59.
[17] C. Sneden, A. McWilliam, G. W. Preston, J. J. Cowan, D. L. Burris, and B. J. Armosky, Astrophys. J. **467**, 819 (1996).
[18] H. R. Jacobson and A. Frebel, J. Phys. G: Nucl. Part. Phys. **41**, 044001 (2014).
[19] P. Barklem, N. Christlieb, T. Beers, V. Hill, M. S. Bessell, J. Holmberg, B. Marsteller, S. Rossi, F.-J. Zickgraf, and D. Reimers, Astron. Astrophys. **439**, 129 (2005).
[20] S. Honda, W. Aoki, Y. Ishimaru, S. Wanajo, and S. G. Ryan, Astrophys. J. **643**, 1180 (2006).
[21] M. Mumpower, R. Surman, G. McLaughlin, and A. Aprahamian, Prog. Part. Nucl. Phys. **86**, 86 (2016).
[22] D. Martin, A. Arcones, W. Nazarewicz, and E. Olsen, Phys. Rev. Lett. **116**, 121101 (2016).
[23] M. Mumpower, T. Kawano, T. Sprouse, N. Vassh, E. Holmbeck, R. Surman, and P. Möller, Astrophys. J. **869**, 14 (2018).
[24] J. Hardy, L. Carraz, B. Jonson, and P. Hansen, Phys. Lett. B **71**, 307 (1977).
[25] B. Rubio, W. Gelletly, E. Nácher, A. Algora, J. L. Taín, A. Pérez, and L. Caballero, J. Phys. G: Nucl. Part. Phys. **31**, S1477 (2005).
[26] D. Jordan, A. Algora, J. L. Taín, B. Rubio, J. Agramunt, A. B. Perez-Cerdan, F. Molina, L. Caballero, E. Nácher, A. Krasznahorkay, M. D. Hunyadi, J. Gulyás, A. Vitéz, M. Csatlós, L. Csige, J. Äysto, H. Penttilä, I. D. Moore, T. Eronen, A. Jokinen, A. Nieminen, J. Hakala, P. Karvonen, A. Kankainen, A. Saastamoinen, J. Rissanen, T. Kessler, C. Weber, J. Ronkainen, S. Rahaman, V. Elomaa, U. Hager, S. Rinta-Antila, T. Sonoda, K. Burkard, W. Hüller, L. Batist, W. Gelletly, A. L. Nichols, T. Yoshida, A. A. Sonzogni, K. Peräjärvi, A. Petrovici, K. W. Schmid, and A. Faessler, Phys. Rev. C **87**, 044318 (2013).
[27] B. C. Rasco, K. P. Rykaczewski, A. Fijałkowska, M. Karny, M. Wolińska Cichocka, R. K. Grzywacz, C. J. Gross, D. W. Stracener, E. F. Zganjar, J. C. Blackmon, N. T. Brewer, K. C. Goetz, J. W. Johnson, C. U. Jost, J. H. Hamilton, K. Miernik, M. Madurga, D. Miller, S. Padgett, S. V. Paulauskas, A. V. Ramayya, and E. H. Spejewski, Phys. Rev. C **95**, 054328 (2017).

[28] A. Gade and S. N. Liddick, J. Phys. G: Nucl. Part. Phys. **43**, 024001 (2016).

[29] W. F. Mueller, B. Bruyneel, S. Franchoo, H. Grawe, M. Huyse, U. Köster, K.-L. Kratz, K. Kruglov, Y. Kudryavtsev, B. Pfeiffer *et al.*, Phys. Rev. Lett. **83**, 3613 (1999).

[30] J. I. Prisciandaro, P. F. Mantica, A. M. Oros-Peusquens, D. W. Anthony, M. Huhta, P. A. Lofy, and R. M. Ronningen, Phys. Rev. C **60**, 054307 (1999).

[31] M. M. Rajabali, R. Grzywacz, S. N. Liddick, C. Mazzocchi, J. C. Batchelder, T. Baumann, C. R. Bingham, I. G. Darby, T. N. Ginter, S. V. Ilyushkin, M. Karny *et al.*, Phys. Rev. C **85**, 034326 (2012).

[32] M. Sawicka, I. Matea, H. Grawe, R. Grzywacz, M. Pfützner, M. Lewitowicz, J. M. Daugas, B. A. Brown, A. Lisetskiy *et al.*, Eur. Phys. J. A **22**, 455 (2004).

[33] S. N. Liddick, W. B. Walters, C. J. Chiara, R. V. F. Janssens, B. Abromeit, A. Ayres, A. Bey, C. R. Bingham, M. P. Carpenter, L. Cartegni, J. Chen, H. L. Crawford, I. G. Darby, R. Grzywacz, J. Harker, C. R. Hoffman, S. Ilyushkin, F. G. Kondev, N. Larson, M. Madurga, D. Miller, S. Padgett, S. V. Paulauskas, M. M. Rajabali, K. Rykaczewski, D. Seweryniak, S. Suchyta, and S. Zhu, Phys. Rev. C **92**, 024319 (2015).

[34] Y. Tsunoda, T. Otsuka, N. Shimizu, M. Honma, and Y. Utsuno, Phys. Rev. C **89**, 031301(R) (2014).

[35] S. Suchyta, S. N. Liddick, Y. Tsunoda, T. Otsuka, M. B. Bennett, A. Chemey, M. Honma, N. Larson, C. J. Prokop, S. J. Quinn, N. Shimizu, A. Simon, A. Spyrou, V. Tripathi, Y. Utsuno, and J. M. VonMoss, Phys. Rev. C **89**, 021301(R) (2014).

[36] C. J. Prokop, B. P. Crider, S. N. Liddick, A. D. Ayangeakaa, M. P. Carpenter, J. J. Carroll, J. Chen, C. J. Chiara, H. M. David, A. C. Dombos, S. Go, J. Harker, R. V. F. Janssens, N. Larson, T. Lauritsen, R. Lewis, S. J. Quinn, F. Recchia, D. Seweryniak, A. Spyrou, S. Suchyta, W. B. Walters, and S. Zhu, Phys. Rev. C **92**, 061302(R) (2015).

[37] B. Crider, C. Prokop, S. Liddick, M. Al-Shudifat, A. Ayangeakaa, M. Carpenter, J. Carroll, J. Chen, C. Chiara, H. David, A. Dombos, S. Go, R. Grzywacz, J. Harker, R. Janssens, N. Larson, T. Lauritsen, R. Lewis, S. Quinn, F. Recchia, A. Spyrou, S. Suchyta, W. Walters, and S. Zhu, Phys. Lett. B **763**, 108 (2016).

[38] F. Recchia, S. M. Lenzi, S. Lunardi, E. Farnea, A. Gadea, N. Mărginean, D. R. Napoli, F. Nowacki, A. Poves, J. J. Valiente-Dobón, M. Axiotis, S. Aydin, D. Bazzacco, G. Benzoni, P. G. Bizzeti, A. M. Bizzeti-Sona, A. Bracco, D. Bucurescu, E. Caurier, L. Corradi, G. de Angelis, F. Della Vedova, E. Fioretto, A. Gottardo, M. Ionescu-Bujor, A. Iordachescu, S. Leoni, R. Mărginean, P. Mason, R. Menegazzo, D. Mengoni, B. Million, G. Montagnoli, R. Orlandi, G. Pollarolo, E. Sahin, F. Scarlassara, R. P. Singh, A. M. Stefanini, S. Szilner, C. A. Ur, and O. Wieland, Phys. Rev. C **85**, 064305 (2012).

[39] I. Stefanescu, D. Pauwels, N. Bree, T. E. Cocolios, J. Diriken, S. Franchoo, M. Huyse, O. Ivanov, Y. Kudryavtsev, N. Patronis, J. VanDeWalle, P. VanDuppen, and W. B. Walters, Phys. Rev. C **79**, 044325 (2009).

[40] D. Morrissey, B. Sherrill, M. Steiner, A. Stolz, and I. Wiedenhoever, Nucl. Instrum. Methods Phys. Res., Sect. B **204**, 90 (2003).

[41] S. N. Liddick, A. Spyrou, B. P. Crider, F. Naqvi, A. C. Larsen, M. Guttormsen, M. Mumpower, R. Surman, G. Perdikakis *et al.*, Phys. Rev. Lett. **116**, 242502 (2016).

[42] A. Spyrou, S. N. Liddick, F. Naqvi, B. P. Crider, A. C. Dombos, D. L. Bleuel, B. A. Brown, A. Couture, L. Crespo-Campo, M. Guttormsen, A. C. Larsen *et al.*, Phys. Rev. Lett. **117**, 142701 (2016).

[43] A. Spyrou, A. C. Larsen, S. N. Liddick, F. Naqvi, B. P. Crider, A. C. Dombos, M. Guttormsen, D. L. Bleuel, A. Couture, L. Crespo Campo *et al.*, J. Phys. G: Nucl. Part. Phys. **44**, 044002 (2017).

[44] A. C. Larsen, J. E. Midtbø, M. Guttormsen, T. Renstrøm, S. N. Liddick, A. Spyrou, S. Karampagia, B. A. Brown, O. Achakovskiy, S. Kamerdzhiev, D. L. Bleuel, A. Couture, L. C. Campo, B. P. Crider, A. C. Dombos, R. Lewis, S. Mosby, F. Naqvi, G. Perdikakis, C. J. Prokop, S. J. Quinn, and S. Siem, Phys. Rev. C **97**, 054329 (2018).

[45] A. Simon, S. Quinn, A. Spyrou, A. Battaglia, I. Beskin, A. Best, B. Bucher, M. Couder, P. DeYoung *et al.*, Nucl. Instrum. Methods Phys. Res., Sect. A **703**, 16 (2013).

[46] A. C. Dombos, D.-L. Fang, A. Spyrou, S. J. Quinn, A. Simon, B. A. Brown, K. Cooper, A. E. Gehring, S. N. Liddick, D. J. Morrissey *et al.*, Phys. Rev. C **93**, 064317 (2016).

[47] M. Birch, B. Singh, I. Dillmann, D. Abriola, T. Johnson, E. McCutchan, and A. Sonzogni, Nucl. Data Sheets **128**, 131 (2015).

[48] C. Mazzocchi, R. Grzywacz, J. Batchelder, C. Bingham, D. Fong, J. Hamilton, J. Hwang, M. Karny, W. Krolas, S. Liddick, A. Lisetskiy, A. Morton, P. Mantica, W. Mueller, K. Rykaczewski, M. Steiner, A. Stolz, and J. Winger, Phys. Lett. B **622**, 45 (2005).

[49] M. Bernas, P. Armbruster, S. Czajkowski, H. Faust, J. P. Bocquet, and R. Brissot, Phys. Rev. Lett. **67**, 3661 (1991).

[50] O. Sorlin, C. Donzaud, L. Axelsson, M. Belleguic, R. Béraud, C. Borcea, G. Canchel, E. Chabanat, J. Daugas, A. Emsallem, D. Guillemaud-Mueller, K.-L. Kratz, S. Leenhardt, M. Lewitowicz, C. Longour, M. Lopez, F. de Oliveira Santos, L. Petizon, B. Pfeiffer, F. Pougheon, M. Saint-Laurent, and J. Sauvestre, Nucl. Phys. A **660**, 3 (1999).

[51] L. Gaudefroy, Etude de la fermeture de couches N = 28: implication astrophysique. Spectroscopie Béta Gamma de noyaux riches en neutrons, Ph.D. thesis, Université Paris Sud-Paris XI, 2005.

[52] J. M. Daugas, I. Matea, J.-P. Delaroche, M. Pfützner, M. Sawicka, F. Becker, G. Bélier, C. R. Bingham, R. Borcea, E. Bouchez, A. Buta, E. Dragulescu, G. Georgiev, J. Giovinazzo, M. Girod, H. Grawe, R. Grzywacz, F. Hammache, F. Ibrahim, M. Lewitowicz, J. Libert, P. Mayet, V. Méot, F. Negoita, F. de Oliveira Santos, O. Perru, O. Roig, K. Rykaczewski, M. G. Saint-Laurent, J. E. Sauvestre, O. Sorlin, M. Stanoiu, I. Stefan, C. Stodel, C. Theisen, D. Verney, and J. Żylicz, Phys. Rev. C **83**, 054312 (2011).

[53] O. Sorlin, C. Donzaud, F. Azaiez, C. Bourgeois, L. Gaudefroy, F. Ibrahim, D. Guillemaud-Mueller, F. Pougheon, M. Lewitowicz, F. de Oliveira Santos, M. Saint-Laurent, M. Stanoiu, S. Lukyanov, Y. Penionzhkevich, J. Angélique, S. Grévy, K.-L. Kratz, B. Pfeiffer, F. Nowacki, Z. Dlouhy, and J. Mrasek, Nucl. Phys. A **719**, C193 (2003).

[54] F. Naqvi, S. Karampagia, A. Spyrou, S. N. Liddick, A. C. Dombos, D. L. Bleuel, B. A. Brown, L. Crespo Campo, A. Couture, B. P. Crider, T. Ginter, M. Guttormsen, A. C. Larsen, R. Lewis, P. Möller, S. Mosby, G. Perdikakis, C. Prokop, T. Renstrøm, and S. Siem (unpublished).

[55] C. Nesaraja, Nucl. Data Sheets **115**, 1 (2014).

[56] K. Abusaleem and B. Singh, Nucl. Data Sheets **112**, 133 (2011).
[57] F. Bečvář, Nucl. Instrum. Methods Phys. Res. A **417**, 434 (1998).
[58] P. Möller, J. Nix, and K.-L. Kratz, At. Data Nucl. Data Tables **66**, 131 (1997).
[59] P. Möller, A. Sierk, T. Ichikawa, and H. Sagawa, At. Data Nucl. Data Tables **109–110**, 1 (2016).
[60] P. Avogadro and T. Nakatsukasa, Phys. Rev. C **84**, 014314 (2011).
[61] M. T. Mustonen, T. Shafer, Z. Zenginerler, and J. Engel, Phys. Rev. C **90**, 024308 (2014).
[62] T. Shafer, J. Engel, C. Fröhlich, G. C. McLaughlin, M. Mumpower, and R. Surman, Phys. Rev. C **94**, 055802 (2016).
[63] M. T. Mustonen and J. Engel, Phys. Rev. C **93**, 014304 (2016).
[64] M. Honma, T. Otsuka, B. A. Brown, and T. Mizusaki, Phys. Rev. C **69**, 034335 (2004).
[65] D. R. Entem and R. Machleidt, Phys. Rev. C **68**, 041001(R) (2003).
[66] ManyBodyPhysics, Manybodyphysics/cens, 2017.
[67] G. Martínez-Pinedo, A. Poves, E. Caurier, and A. P. Zuker, Phys. Rev. C **53**, R2602(R) (1996).
[68] J. L. Tain, E. Valencia, A. Algora, J. Agramunt, B. Rubio, S. Rice, W. Gelletly, P. Regan, A.-A. Zakari-Issoufou, M. Fallot, A. Porta, J. Rissanen, T. Eronen, J. Äystö, L. Batist, M. Bowry, V. M. Bui, R. Caballero-Folch, D. Cano-Ott, V.-V. Elomaa, E. Estevez, G. F. Farrelly, A. R. Garcia, B. Gomez-Hornillos, V. Gorlychev, J. Hakala, M. D. Jordan, A. Jokinen, V. S. Kolhinen, F. G. Kondev, T. Martínez, E. Mendoza, I. Moore, H. Penttilä, Z. Podolyák, M. Reponen, V. Sonnenschein, and A. A. Sonzogni, Phys. Rev. Lett. **115**, 062502 (2015).
[69] M. Wiedeking, M. Krtička, L. A. Bernstein, J. M. Allmond, M. S. Basunia, D. L. Bleuel, J. T. Burke, B. H. Daub, P. Fallon, R. B. Firestone, B. L. Goldblum, R. Hatarik, P. T. Lake, A. C. Larsen, I.-Y. Lee, S. R. Lesher, S. Paschalis, M. Petri, L. Phair, N. D. Scielzo, and A. Volya, Phys. Rev. C **93**, 024303 (2016).
[70] J. C. Hardy and I. S. Towner, Phys. Rev. C **79**, 055502 (2009).
[71] W.-M. Y. *et al.*, J. Phys. G: Nucl. Part. Phys. **33**, 1 (2006).
[72] N. Gove and M. Martin, At. Data Nucl. Data Tables **10**, 205 (1971).